STUDIA INFORMATICA
Nr 1-2 (22) Systems and information technology 2018

Paweł M. STANO

Department of Complex Systems,
National Centre for Nuclear Research,
ul. A. Sołtana 7, 05–400 Otwock-Świerk, Poland

The collapse of sequential Bayesian estimator in two-target tracking problem

Abstract. Track coalescence is a phenomenon that occurs in multi-target tracking applications where certain types of manoeuvres performed simultaneously by several targets can utterly confuse algorithms that track their positions. In its simplest form, the phenomenon occurs when two similar objects, initially well separated, get close to each other and follow similar manoeuvres for a period of time sufficient to confound the tracking algorithm so that when the objects finally depart from each other the tracking algorithm is prone to provide erroneous estimates. This two-target track coalescence is discussed in this paper with the focus on the compound coalescence, when two identical tracks follow the midpoint of two well separated targets. First, the problem is illustrated on a classic problem of tracking two targets manoeuvring in a clutter, which is modeled as a nonlinear stochastic system. It is shown how, otherwise accurate and precise, estimates obtained by a standard particle filter eventually collapse leading to the coalescence of tracks. The phenomenon is given theoretical explanation by the analysis of Bayesian update operator acting on L2-space of probability densities that reveals that the coalescence is an unavoidable consequence of the probabilistic mixing between distributions describing positions of two targets. Finally, the practical consequences of these theoretical results are discussed together with potential approaches to deal with track coalescence in real applications.

Keywords. Track coalescence, Bayesian operator, target tracking, particle filter

1. Introduction

Target tracking is a subject extensively studied in the stochastic dynamical systems theory and practice. The classical formulation of the problem can be found in [1], where the Kalman derived an optimal solution for linear and Gaussian tracking problem, which is known as Kalman Filter. In case of nonlinear and/or non-Gaussian tracking problems no optimal solution exists in a closed analytical form. Instead, one needs to rely on approximate solutions, which can be divided into parametric and non-parametric filters. There exists a plethora of algorithms in each of these group. The parametric methods are based on analytical approximations of nonlinear system dynamic (e.g., Extended Kalman Filter [2]), statistical approximations of system uncertainty (e.g., Unscented Kalman Filter [3]) or the combination of both (e.g., Gaussian Sum Filter [4]). An extensive survey on the subject of parametric filters is presented in [5]. These algorithms are, in general, simple to implement and computationally inexpensive, which makes them very popular in applications requiring online high-frequency estimates. On the other hand, the parametric methods are rather rigid and thus prone to approximation errors, especially in the presence of severe nonlinearities in the system. To deal with such situations, the non-parametric Particle Filters (PF) have been developed. These algorithms approximate the probability distribution function (pdf) of the state of the system by a large set of weighted points (particles) that, in theory, can fit a pdf of any arbitrary shape [6]. The PF produces better estimates but the price for accuracy is significantly higher computational load of the algorithm when compared to parametric methods.

In this paper the properties of Bayesian estimator used to track positions of two manoeuvring targets in a clutter shall be discussed in the context of a phenomenon commonly known as track coalescence [7, 8]. This is a well-known problem in target tracking applications and usually occurs when two similar object, initially well separated, get close to each other and follow similar manoeuvres for a period of time sufficient to confuse the tracking algorithm so that when the objects finally depart from each other the tracking algorithm is prone to provide erroneous estimates. Several types of errors associated with track coalescence can be distinguished: misalignment, when track switch the targets they follow; simple coalescence, when two identical tracks follow a single target; and compound coalescence, when two identical tracks follow the midpoint of two well separated targets. The focus of this paper is to discuss only the latter phenomenon of compound track coalescence.

To do that, first in Section 2 a classic example of targets manoeuvring in a clutter is defined. Next, in Section 3 a typical example of track coalescence is presented for a system using the standard PF. Furthermore, it is shown how, after following close trajectories for some time, the initially well separated distributions of targets mix to the point they become

indistinguishable from each other. Next, in Section 4 through analysis Bayesian update operator acting on L2-space of probability densities, the coalescence is presented as an unavoidable consequence of the probabilistic mixing between distributions describing the positions of two targets. Section 5 concludes the paper by discussing various approaches to deal with the track coalescence.

2. Two-target tracking in a clutter problem

In this section the two-target tracking problem is defined and some of its properties are discussed. For the sake of clarity, the problem is presented in a simple classic formulation where the relative distance between the targets is the only dimension that matters. Nevertheless, the properties discussed in this paper are applicable to general target tracking systems.

A common approach is to model two-target tracking problem as nonlinear stochastic dynamic system, where the states of both targets $x_k^i = \left[x_{pos}^i, x_{vel}^i\right]_k^T, i = 1,2$, correspond to target position x_{pos} and velocity x_{vel} at time step *k*. The system equations are as follows [9]:

$$x_k^i = A_i x_{k-1}^i + w_k^i \quad (1a)$$
$$z_k^i = H_i x_k^i + g_i v_k^i \quad (1b)$$

where: A_i, H_i are system matrices that model state evolution $\{x_t^i\}_{t=1}^k$ and observation process $\{z_t^i\}_{t=1}^k$, respectively; $\{v_t^i\}_{t=1}^k$ is a sequence of independent identically distributed (i.i.d.) standard Gaussian variables that, after multiplication by a g_i factor (scalar value), model the observation noise; and $\{w_t^i\}_{t=1}^k$ is a sequence of i.i.d. Gaussian variables with time-invariant covariance matrix

$$W_i \coloneqq \begin{bmatrix} T_s^3/3 & T_s^2/2 \\ T_s^2/2 & T_s \end{bmatrix} \quad (2)$$

where T_s is the sampling time.

For simplicity let us assume that the models for both targets are equal, i.e., that for *i = 1, 2* the matrices A_i, H_i are given by

$$A_i \coloneqq \begin{bmatrix} 1 & T_s \\ 0 & 1 \end{bmatrix}, \quad (3)$$

$$H_i \coloneqq [1 \quad 0] \quad (4)$$

and that $g_i = g$ for *i = 1, 2*.

Remark 2.1 (dimensionality) Note that matrices W_i, A_i, H_i describe the dynamics of target position and velocity so the state vector of each target can be decomposed into $x_k^i = \left[x_{pos}^i, x_{vel}^i\right]_k^T$. The actual dimension of the vector x_k^i depends on a particular problem being modelled, e.g., if the system model airborne objects, the state position is three-dimensional; in case of ground vehicles moving at a at surface the state position would be two-dimensional; on the other hand if the modeller is concerned only with the relative position between two targets, the state position is one-dimensional. In general, for n_{pos} – the dimension of state position and n_{vel} - the dimension of state velocity, the dimensions of matrices W_i, A_i, H_i are equal to $\left(n_{pos} + n_{vel}\right) \times \left(n_{pos} + n_{vel}\right)$, $\left(n_{pos} + n_{vel}\right) \times \left(n_{pos} + n_{vel}\right)$, $\left(n_{pos} +\right.$ *nvel×npos*, respectively.

So far, the system dynamics for marginal targets is linear. The dynamical system for the joined two-targets state $x_k = [x_k^1, x_k^2]_k^T$ and the joined observation $z_k = [z_k^1, z_k^2]_k^T$ is then given by

$$x_k = \begin{bmatrix} A_1 & 0 \\ 0 & A_2 \end{bmatrix} x_{k-1} + \begin{bmatrix} w_k^1 \\ w_k^2 \end{bmatrix}, \quad (5)$$

$$z_k = \begin{bmatrix} H_1 & 0 \\ 0 & H_2 \end{bmatrix} x_k + \begin{bmatrix} g & 0 \\ 0 & g \end{bmatrix} \begin{bmatrix} v_k^1 \\ v_k^2 \end{bmatrix}. \quad (6)$$

At each time step *k* we collect the measurement vector $y_k = [y_k^1, y_k^2]^T$ however without knowing from which target y_k^1 and y_k^2 originate. However, we know that the measurement vector y_k is related to the state system by

$$\underline{\chi_k} y_k = z_k, \quad (7)$$

where $\underline{\chi_k} := \chi_k \otimes I$, with $\{\chi_t\}_{t=1}^k$ is a sequence of i.i.d. random 2×2 permutations so that $\underline{\chi_k}$ takes values *I* or Π, which are defined as:

$$I = \begin{bmatrix} 1 & 0 \\ 0 & 1 \end{bmatrix}, \quad (8)$$

$$\Pi = \begin{bmatrix} 0 & 1 \\ 1 & 0 \end{bmatrix}. \quad (9)$$

The data association uncertainty defined by (7) introduces nonlinearity to the otherwise linear model. The conditional probability distribution $p_{x_k|y_k}$ of the state x_k given the measurements y_k is given by [9]:

$$p_{x_k|y_k}(x) = \frac{1}{c_k}\sum_{\chi\in\{I,\Pi\}} N\left(\underline{\chi_k} y_k; \tilde{H}x, \tilde{G}\tilde{G}^T\right) \int_{\mathbb{R}^{2n}} N\left(x; \tilde{A}x', \tilde{W}\right) p_{x_{k-1}|y_{k-1}}(x')dx', \quad (10)$$

where c_k is a normalizing constant, $n = n_{pos} + n_{vel}$ is the dimension of the state vector (composed position and velocity of the target), and

$$\tilde{A} \coloneqq \begin{bmatrix} A & 0 \\ 0 & A \end{bmatrix}, \quad (11)$$

$$\tilde{H} \coloneqq \begin{bmatrix} H & 0 \\ 0 & H \end{bmatrix}, \quad (12)$$

$$\tilde{G} \coloneqq \begin{bmatrix} g & 0 \\ 0 & g \end{bmatrix}, \quad (13)$$

$$\tilde{W} \coloneqq \begin{bmatrix} W & 0 \\ 0 & W \end{bmatrix}. \quad (14)$$

The objective of two-target tracking problem is to estimate the posterior density (10) given the initial a priori distribution p_0 and consecutive measurements y_k.

3. Track coalescence phenomenon

In this section a typical example used to illustrate the phenomenon of track coalescence is discussed. This example consists of two targets, which manoeuvre according to the dynamics described in Section 2, and that are followed by tracking algorithm estimating target positions from noisy measurements. In this example only the relative distance between the targets is of importance, hence the state position of both targets is one-dimensional. The tactical manoeuvres of both targets are planned in three stages:

The systems is initiated with two well-separated targets that start moving towards each other (stage 1: separation). During this phase, the tracking algorithm follows both targets with desired accuracy and precision.

After the targets get sufficiently close, they maintain a fixed distance from each other while moving with equal velocity on parallel trajectories (stage 2: mixing). During the second phase the tracking algorithm becomes increasingly less accurate and precise. Typically, the

estimated positions of both targets are located somewhere between their true positions. Nevertheless, as targets are close to each other, the estimation bias is not significant.

Finally, after enough time has passed to allow strong mixing of posterior distributions, both targets depart from each other (stage 3: coalescence). In this phase the tracking algorithm is completely confused about the location of both targets, with fifty-fifty chances of assigning to each of them. In a typical situation, as the tracking algorithm cannot decide which target to follow, the track is stuck half way between both targets, which leads to a significant estimation bias. Such situation might prevail for a long time after the departure happened but typically as the time passes the estimation bias diminishes as the tracking algorithm catches the trail of escaping targets. Unfortunately, this can be a very slow process and there is half-half probability that the algorithm assigns tracks to wrong targets.

The situation described above is visualised by simulations inspired by [9], which are presented in Figure 3.1, the trajectories of two targets are presented together with noisy measurements of their relative positions. The relative distances between the targets are rescaled so that their initial positions are *1* and *-1*, respectively. In this scale, the noise of the measurements is equal to $g = 0.06$.

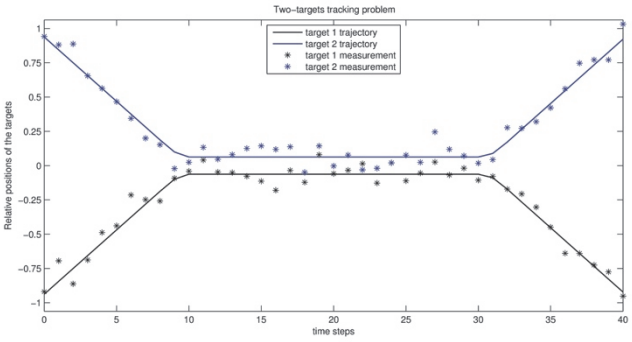

Figure 3.1. Two-targets tracking system. The solid lines represent the trajectories of both targets while the stars represent noisy measurements associated with them.

The simulation starts with the targets being well-separated (stage 1) in the eyes of the tracking algorithm, i.e., the prior probabilities of target positions are described by Gaussian distribution with standard deviation $\sigma = 0.06$ and means equal to *1* and *-1*, respectively. At time step 10, after the distance between the targets is reduced to 0.1 (5% of the initial distance), the mixing phase (stage 2) of the simulation begins. This phase lasts until time step 30 when the targets separate (stage 3) to return to their initial relative distance.

Given that the system described above is nonlinear, a nonlinear nonparametric tracking algorithm, namely Sample Importance Resampling Particle Filter [10] (SIR PF), is used to estimate its states.

The SIR PF is a nonlinear filtering algorithm used to estimate the states of discrete-time dynamical systems, such as the one defined by (1). The SIR PF approximates the posterior density $p_{k|k}$ of the state x_k by N random samples (particles) $\{x_{k,i}\}_{i=1}^{N}$ and their corresponding weights $\{\omega_{k,i}\}_{i=1}^{N}$, which are normalized to sum to unity. The particles are obtained using the Sequential Importance Sampling (SIS) method [6,11], which is a recursive algorithm that uses the most recent observation y_k to compute the distribution of the state x_k via Bayes rule. The posterior density $p_{k|k}$ is represented by the set of weighted samples in the following way:

$$p_{k|k} \approx p_{k|k}^{N} \coloneqq \sum_{i=1}^{N} \omega_{k,i}\delta_0(x_k - x_{k,i}), \qquad (15)$$

where δ_0 denotes the Dirac delta at zero. Over the last years, PFs have gained much popularity in the nonlinear filtering community because their flexibility allows them to be applied to large variety of systems. In this paper the most basic SIR PF is used, which is also known as Bootstrap Particle Filter [12]. The reader interested in more specialised modification of the basic SIR PF is referred to [10, 13, 14, 15].

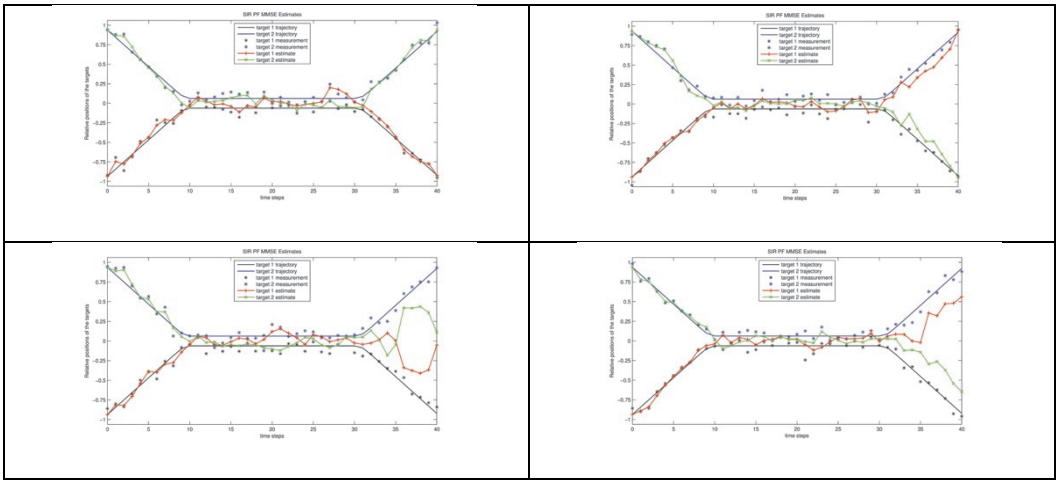

Figure 3.2. Four random realizations of the SIR PF tracking. Depending on a particular random realization of measurement noises the tracks: follow the targets correctly (top left), swap targets (top right), collapse at the mid-point (bottom left), collapse and swap targets (bottom right).

Using the SIR PF to track targets following manouvres described in Figure 3.1 results in typical track coalescence during the last third stage of the simulations. This can be seen in Figure 3.2 where four random realizations of the tracking algorithm are shown (each for particular random realization of measurement noises).

Note that the track coalescence is not due to a choice of the point estimate (MMSE in case of Figure 3.2) nor due to a particular choice of the tracking algorithm (SIR PF in case of Figure 3.2) but it is a consequence of the shape of the posterior distribution. Detailed discussion on this subject is given in the next section, but the phenomenon is visualised in Figure 3.3 and Figure 3.4, which show the evolution of posterior distributions of target 1 and target 2, respectively.

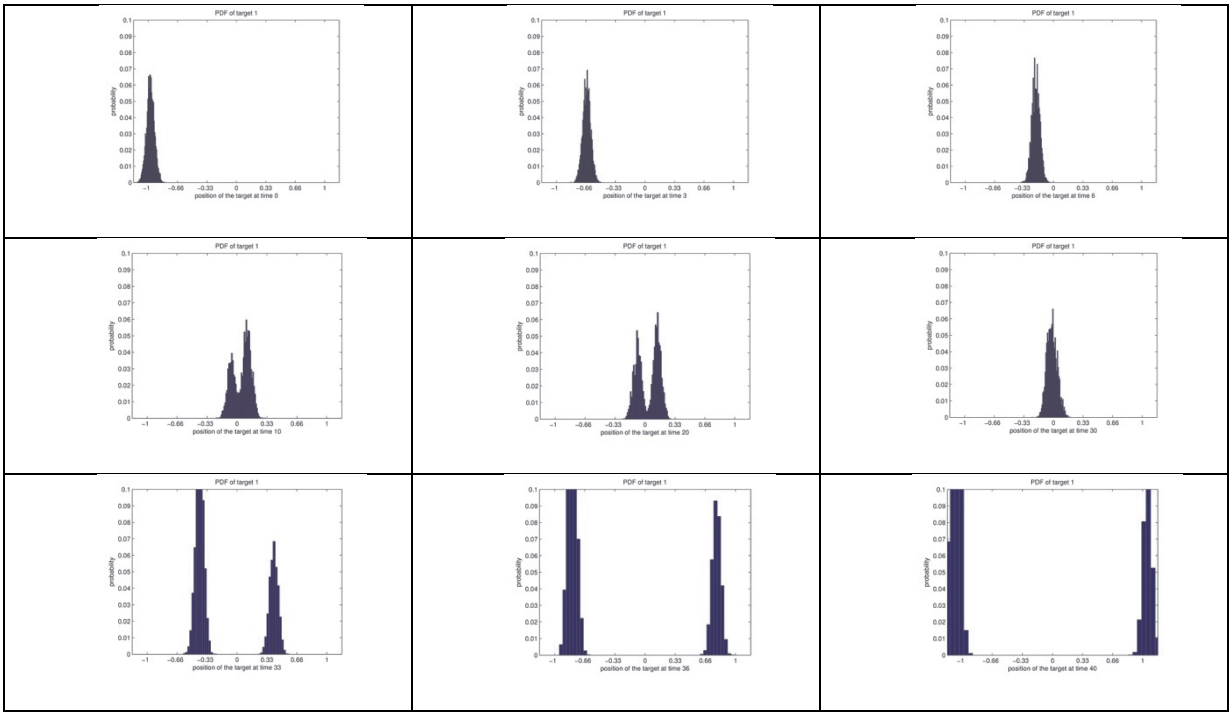

Figure 3.3. The evolution of the posterior distribution of the position of target 1 obtained with the SIR PF. Top row shows how the posterior distribution evolves during the separation stage, the evolution during the mixing stage is presented in middle row, and the evolution of the distribution during the coalescence stage is presented in the bottom row.

It can be seen that at the beginning of the simulation the probability distributions of both targets are centered around their respective positions, and thus well-separated. During the mixing phase, the posterior distribution of both targets converge to each other and center around the symmetry axis between the targets (position 0), while simultaneously the variance of the distribution increases. During the last phase the posterior distributions of both targets remain similar, by each becoming binomial with modes centered around the positions of distant targets. Thus, the posterior distributions are confused about the true locations of both targets and the choice of point estimate cannot prevent the coalescence of tracks.

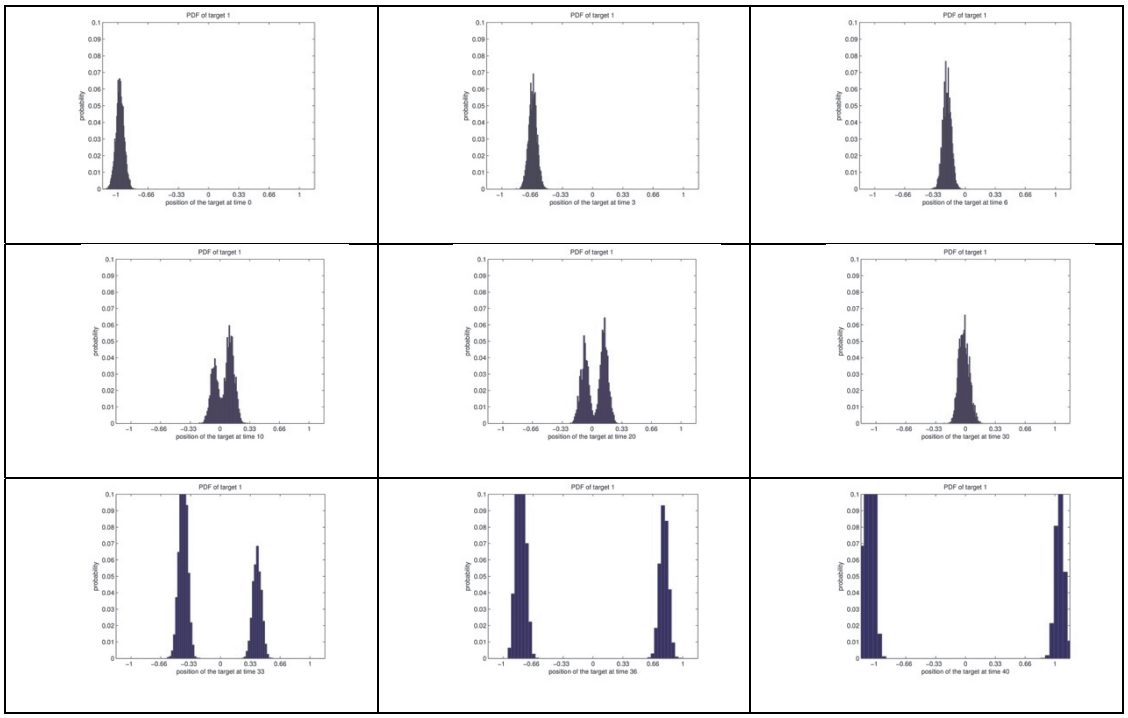

Figure 3.4. The evolution of the posterior distribution of the position of target 2 obtained with the SIR PF. Top row shows how the posterior distribution evolves during the separation stage, the evolution during the mixing stage is presented in middle row, and the evolution of the distribution during the coalescence stage is presented in the bottom row.

4. The source of track coalescence: collapse of Bayesian update operator

In this section the track coalescence phenomenon described in the previous section is shown to be a consequence of the full mixing of the state distribution obtained by sequential application of the Bayesian update. This is done by analyzing the Bayesian operator acting on L2 space of probability densities defined below.

Definition 4.1 (Bayesian update operator [13]) Let us denote the transformation that takes $p_{x_{k-1}|y_{k-1}}$ into $p_{x_k|y_k}$ defined in (10) by $\mathcal{B}$, i.e.,

$$\mathcal{B}_{y_k}\left(p_{x_{k-1}|y_{k-1}}\right) \coloneqq p_{x_k|y_k}. \qquad (16)$$

The first observation about the operator defined by (16) is that it maps a Gaussian prior distribution into a Gaussian-sum posterior distribution. This is formulated formally in Proposition 4.1 below.

Proposition 4.1 Assume that p_0 is a Gaussian distribution defined by

$$p_0(x) \coloneqq N\left(x; \tilde{\mu}, \tilde{\Sigma}\right). \qquad (17)$$

then, the result of applying the Bayesian update operator defined in (10) to p_0 and to the measurement $y = [y^1, y^2]^T$, is a Gaussian-sum distribution.

Proof The proof follows from simple algebra and basic properties of Gaussian distribution. Indeed, after Bayesian update the posterior density is given by:

$$\mathcal{B}_y(p_0)(x) = \frac{1}{c}\left(N(y; \tilde{H}x, \tilde{G}) + N(\Pi y; \tilde{H}x, \tilde{G})\right) \int_{\mathbb{R}^{2n}} N(x; \tilde{A}x', \tilde{W}) p_0(x') dx'$$

$$= \frac{1}{c}\left(N(\tilde{H}x; y, \tilde{G}) N(x; \tilde{A}\tilde{\mu}, \tilde{A}\tilde{\Sigma}\tilde{A}^T + \tilde{W}) + N(\tilde{H}x; \Pi y, \tilde{G}) N(x; \tilde{A}\tilde{\mu}, \tilde{A}\tilde{\Sigma}\tilde{A}^T + \tilde{W})\right).$$

To complete the proof it is enough to observe that the product of two Gaussian densities is also a Gaussian density. Thus, the posterior becomes a binomial Gaussian-sum density.

■

Directly from Proposition 4.1 the following invariance property can be inferred.

Corollary 4.1 The Bayesian update operator defined in (10) is an invariant operator on the sub-space of L2 composed of Gaussian-sum densities.

Proof The proof of Corollary 4.1 follows by Proposition 4.1 and the fact that Bayesian update operator is linear on L2. ■

The second observation about the operator defined by (16) is that it maps a symmetric Gaussian-sum prior distribution into a symmetric Gaussian sum posterior distribution. More precisely, for the Bayesian update operator the following holds.

Proposition 4.2 Let us define the set of symmetric Gaussian-sum densities by:

$$\mathcal{M} := \left\{ \sum_{j=1}^{N} \left(\frac{1}{2N} N(x; \mu_j, \Sigma_j) + \frac{1}{2N} N(x; \Pi\mu_j, \Sigma_j) \right) : \mu_j, \Sigma_j, N \right\} \quad (18)$$

with $\mu_j \in \mathbb{R}^{2n}$, symmetric matrices Σ_j of dimension $2n \times 2n$, and numbers $N \in \mathbb{N}$. Then, for any measurement vector $y \in \mathbb{R}^{2m}$, and state vector $x \in \mathbb{R}^{2n}$, the set $\mathcal{M}$ is invariant with respect to the operator $\mathcal{B}_y(\cdot)$, i.e.,

$$\mathcal{B}_y(\mathcal{M}) \subset \mathcal{M}. \quad (19)$$

Proof To prove Proposition 4.2 it is enough to show that the Bayesian update operator maps a symmetric binomial Gaussian-sum prior density into a symmetric Gaussian-sum posterior density. Thus, let the prior density p_0 be defined as follows:

$$p_0 \coloneqq \frac{1}{2N} N\left(x; \mu, \tilde{\Sigma}\right) + \frac{1}{2N} N\left(x; \Pi\mu, \tilde{\Sigma}\right), \qquad (20)$$

where the means and covariances of the Gaussian densities are given by $\mu = [\mu^1, \mu^2]^T$ and $\tilde{\Sigma} = \begin{bmatrix} A\Sigma A^T + W & 0 \\ 0 & A\Sigma A^T + W \end{bmatrix}$, respectively. Then, for any measurement vector $y = [y^1, y^2]^T$ and two-target state vector $x = [x^1, x^2]^T$, and covariance matrix $\Lambda = \begin{bmatrix} \tilde{A}\tilde{\Sigma}\tilde{A}^T + \widetilde{W} & 0 \\ 0 & \tilde{A}\tilde{\Sigma}\tilde{A}^T + \widetilde{W} \end{bmatrix}$, the posterior density is given by:

$$\mathcal{B}_y(p_0)(x) = \frac{1}{c}\left(N(y; \tilde{H}x, \tilde{G}) + N(\Pi y; \tilde{H}x, \tilde{G})\right) \int_{\mathbb{R}^{2n}} N(x; \tilde{A}x', \widetilde{W}) p_0(x') dx' \approx N(\tilde{H}x, y, \tilde{G}) N(x; \tilde{A}\mu, \Lambda) \quad (21a)$$

$$+N(\tilde{H}x, y, \tilde{G}) N(x; \Pi\tilde{A}\mu, \Lambda) \qquad (21b)$$

$$+N(\tilde{H}x, \Pi y, \tilde{G}) N(x; \tilde{A}\mu, \Lambda) \qquad (21c)$$

$$+N(\tilde{H}x, \Pi y, \tilde{G}) N(x; \Pi\tilde{A}\mu, \Lambda), \qquad (21d)$$

where '≈' means equality up to a normalizing constant.

By the previously recalled properties of Gaussian distribution, the resulting posterior density belongs to a class of Gaussian-sum densities. Furthermore, the structure of the posterior density is such that:

the covariance matrices are symmetric and diagonal (between targets x^1 and x^2),

the means in term (21a) are symmetric to means in term (21d),

the means in term (21b) are symmetric to means in term (21c).

Thus, from points 1.-3. it follows that the posterior density $\mathcal{B}_y(p_0)$ is a symmetric Gaussian-sum density with four components. Hence, the operator (16) maps symmetric binomial Gaussian densities into $\mathcal{M}$. To finish the proof it is enough to observe that any function $p \in \mathcal{M}$ is composed of several symmetric binomial Gaussians p_i and that the operator $\mathcal{B}_y(\cdot)$ is additive. Thus

$$\mathcal{B}_y(p) = \mathcal{B}_y(\textstyle\sum_i p_i) = \frac{1}{c}\sum_i \mathcal{B}_y(p_i) \in \mathcal{M} \qquad (22)$$

where c is a normalizing constant. ■

So far, the discussion was focused on properties of Bayesian operator that dynamically maps prior distribution into posterior distribution. However, in typical tracking applications

one is eventually interested in obtaining a point estimate of target position. This value can be derived from the posterior distribution by applying a point estimator to the posterior pdf. The most common point estimators are those that solve either of the following optimization problem:

minimize the mean square error between the posterior pdf and the true unknown state;

maximize the likelihood of the posterior pdf.

The solution to the former optimization problem, the Minimal Mean Square Error (MMSE) estimator is provided by an expected value, whereas the solution to the latter problem, the Maximum A Posteriori Probability (MAP) estimator is given by mode of the posterior pdf [5]. In the reminder of this section it is discussed how these two point estimators behave when applied to densities belonging to the invariant set $\mathcal{M}$.

Corollary 4.2 For any prior symmetric Gaussian-sum density $p_0 \in \mathcal{M}$ the MMSE estimator applied to the Bayesian posterior $\mathcal{B}_y(p_0)(\cdot)$ will always lead to a perfect coalescence of target tracks.

Proof To prove Corollary 4.2 it is sufficient to note that

the MMSE estimator is given by the expectation of the posterior distribution,

the expectation of the distribution defined by (4) is symmetric, i.e

$$\mathcal{E}(x^1) = \int x^1 \mathcal{B}_y(p)(x^1)dx^1 = \int x^2 \mathcal{B}_y(p)(x^2)dx^2 = \mathcal{E}(x^2), \qquad (23)$$

where $\mathcal{E}(x^1)$ denotes expected value of the variable x^1. ■

Thus, it has been shown that the track coalescence of the two-targets tracking system based on MMSE estimator is a consequence of the persistent symmetry existing in the system from the moment it enters the subspace $\mathcal{M}$.

Corollary 4.3 For any prior symmetric Gaussian-sum density $p_0 \in \mathcal{M}$ the MAP estimator applied to the Bayesian posterior $\mathcal{B}_y(p_0)(\cdot)$ will always lead to track coalescence or to random misalignment of tracks.

Proof The corollary is again a consequence of the persistent symmetry existing in the system. The coalescence of MAP estimates happens when the a posteriori Gaussian-sum density has its mass centred around symmetry axis (0, 0), whereas the random misalignment

of the MAP estimates occur when the a posteriori Gaussian-sum density resembles the binomial distribution with mass divided equally among the position of both targets. ■

5. Discussion

In the previous sections it has been shown that if two targets stay sufficiently close and for sufficiently long period of time the joint tracking distribution of both targets become symmetric. As a consequence, both targets become indistinguishable from each other. Furthermore, once the state of symmetry is achieved it persists even if after some time both targets depart far away from each other. The final point estimates of targets positions, such as those obtained from MMSE or MAP statistics, are derived from the joint posterior distribution. Due to inherent symmetry of the underlying distribution, such estimates result in track coalescence if the mean value of the distribution is taken (MMSE estimator) or to either coalescence or random alignment of tracks when maximum likelihood estimators are used (MAP estimator).

In the theoretical case of ideally symmetrical prior distribution it is impossible to escape the symmetry following the sequential Bayesian estimation only, nor it is possible to avoid track coalescence or track misalignment by construction of other specialized point estimates. In the real applications the perfect symmetry is never achieved. Instead, after long enough mixing, the joint distribution of target states is composed of dominant symmetric part and residual asymmetric part. The former component preserves its symmetry accordingly to the theory described in previous section. During the mixing stage of the process, the latter asymmetric component acts similarly to a random walk with covariances defined by noises of the system (1), i.e., by covariance matrices W and G. After the mixing stage is over, i.e., after the targets depart from each other, the asymmetric component will eventually become dominant over its symmetric counterpart, which in consequence will lead to breaking of the symmetry of the posterior distribution. Unfortunately, this can be very slow process due to the fact that realizations of random walk can oscillate around the symmetry axis for a long time. Furthermore, due to randomness of the asymmetric component, there is no guarantee that after the symmetry is broken, the tracks will follow correct targets. In reality, when the symmetry is finally broken there is fifty-fifty chance of misalignment of target tracks. For other algorithms that exploit the asymmetric component in the tracking algorithms the reader is referred to [8, 9,16,17].

When considering the choice of the point estimates it is important to note that the MMSE estimate is more prone to track coalescence than the MAP estimate. This is because it takes a lot of time for the asymmetric component to shift the expectation of the posterior distribution to the place where it matches the actual positions of the targets. The MAP estimate is

immediately affected by the asymmetry as it follows the track with even slightly larger probability mass. On the other side, the MMSE estimate is more stable in target tracking, whereas the MAP estimate frequently jumps from one target to another as the asymmetric component randomly oscillates around the symmetry axis. Regardless of the choice of point estimates, the misalignment of target tracks cannot be effectively avoided as it is a consequence of the previously described collapse of sequential Bayesian operator.

References

1. Kalman, R. E.: A new approach to linear filtering and prediction problems, Journal of basic Engineering, vol. 82, pp. 35-45, 1960.

2. Ljung, L.: Asymptotic behavior of the extended Kalman filter as a parameter estimator for linear systems. IEEE Transactions on Automatic Control, vol. 24, pp. 36-50, 1979.

3. Wan E. A., Van Der Merwe R.: The unscented Kalman filter for nonlinear estimation. In Adaptive Systems for Signal Processing, Communications, and Control Symposium (AS-SPCC), pp. 153-158, 2000.

4. Alspach D. L., Sorenson H., Recursive Bayesian Estimation Using Gaussian Sums, Automatica, vol. 7, pp. 465–479, 1971.

5. Stano, P. M., Lendek, Zs., Braaksma, J., Babuska, R., de Keizer, C., den Dekker, A, J. Parametric Bayesian filters for nonlinear stochastic dynamical systems: A survey. IEEE transactions on cybernetics, vol. 43, pp. 1607-1624, 2013.

6. Arulampalam S., Maskell S., Gordon N., Clapp T.: A Tutorial on Particle Filters for Online Nonlinear/Non- Gaussian Bayesian Tracking, IEEE Transactions on Signal Processing, issue 50, pp. 174-188, 2002.

7. Blom H. A., Bloem E. A.: Optimal Decomposed Particle Filtering of Two Closely Spaced Gaussian Targets, Proceedings of the IEEE Conference on Decision and Control and European Control Conference (CDC-ECC), pp. 7895-7901, 2011.

8. Blom H. A., Bloem E. A., Musicki, D.: JIPDA: Automatic Target Tracking Avoiding Track Coalescence, IEEE Transactions on Aerospace and Electronic Systems, vol. 51, pp. 962-974, 2015.

9. Blom H. A., Bloem E. A.: Decomposed Particle Filtering and Track Swap Estimation in Tracking Two Closely Spaced Targets, Proceedings of the 14th International Conference on Information Fusion (FUSION), pp. 1-8, 2011.

10. Ristic B., Arulampalam S., Gordon N.: Beyond the Kalman Filter: Particle Filters for Tracking Application. Artech House, 2004.

11. Doucet A., Godsill S., Andrieu, Ch.: On Sequential Monte Carlo Sampling Methods for Bayesian Filtering, Statistics and Computing, vol. 10, pp. 197-208, 2000.

12. Stano P. M., Tilton A. K., Babuska R.: Estimation of the Soil-dependent Time-varying Parameters of the Hopper Sedimentation Model: The FPF versus the BPF, Control Engineering Practice, vol. 24, pp. 67-78, 2014.

13. Stano P. M., Lendek Zs., Babuska R.: Saturated Particle Filter: Almost Sure Convergence and Improved Resampling, Automatica, vol. 49, pp. 147-159, 2013.

14. Stano P. M., den Dekker, A. J., Lendek Zs., Babuska R.: Convex Saturated Particle Filter, Automatica, vol. 50, pp. 2494-2503, 2014.

15. Yang T., Blom H. A., Mehta P. G.: Interacting Multiple Model-Feedback Particle Filter for Stochastic Hybrid Systems, Proceedings of the IEEE Annual Conference on Decision and Control (CDC), pp. 7065-7070, 2013.

16. Svensson L., Svensson D., Guerriero M., Willett P.: Set JPDA Filter for Multitarget Tracking, IEEE Trans. Signal Process, vol. 59, pp. 4677–4691, 2011.

17. Chen X., Li Y., Li Y., Yu J., Li, X.: A Novel Probabilistic Data Association for Target Tracking in a Cluttered Environment, Sensors, vol. 16, pp. 2180, 2016.